



Physico-Mechanical Characteristics of Reinforced Slag-Based Geopolymer Composites by Using Steel Fibers

S.Abd elmoied¹, Hisham Khater², Tarek Osman², Fouad Elhosiny³, Ramadan M. Ramadan⁴

¹ Housing and Building National Research Center, Faculty of Science, Ain Shams University, Egypt

² Professor at Housing and Building National Research center HBRC, Cairo, Egypt

³ Professor of Physical Chemistry, Ain Shams University, Cairo, Egypt

⁴ Professor of Inorganic Chemistry, Ain Shams University, Cairo, Egypt

Abstract

A considerable portion of the CO₂ emissions produced during the cement manufacturing process contribute to the greenhouse effect and the planet's warming. This prompted the quest for cement substitutes that were more environmentally friendly. Utilizing steel slag from blast furnaces or creating slag geopolymer composites are good alternatives. Despite having good compressive strength and endurance, blastfurnace steel slag in geopolymer has low flexural and tensile strength. In order to address these issues, steel fibres are introduced. This study examines the effects of adding steel fibres to slag-based geopolymer composites that have been activated by an alkaline solution of 6 % sodium hydroxide in various ratios (0.5, 1, 2, and 3 percent by weight). Compressive strength, water/binder ratio, and mechanical characteristics are described. Several methods, including X-ray diffraction and Fourier transform infrared spectra, have been used to pinpoint the phases and structural characteristics of the resulting geopolymer. The results demonstrated that adding different percentages of steel fibre up to 2 % followed by a step decrease, led to higher mechanical strength, shrinkage, water absorption, crack propagation, and post-cracking in the resulting geopolymer composites.

Keywords: Geopolymer; composites; slag; steel fiber; sustainable materials; X-ray diffraction Physico-mechanical characteristics ; Fourier transform infrared spectra .

1. Introduction

Intensive research has been done and is still being done to produce alkali-activated binders (Geopolymers), implying that such a novel binder could have a huge potential in cement binders. Geopolymers having low energy consumption as well as low CO₂ emission have been discovered in 1978 by Joseph Davidovits [1,2]. Geopolymers could be synthesized using alkali-activation of alumino-silicate materials [3-5] for example: Kaolinite clays, metakaolin, fly ash, blastfurnace steel slag. Several studies have found that this novel material (geopolymer) has advantages over traditional materials, such as lower raw material costs and an environmentally friendly manufacturing process. Geopolymers have a number of useful physical and engineering features, including strong temperature resistance, UV resistance, high compressive strength, and long-term durability [6,7]. In addition to their

excellent mechanical and durability aspects, several researchers indicated that Geopolymers possess excellent interfacial adhesion and durability [8,9]. Geopolymers have been used in several applications, for example, masonry structures, repair materials [10], coating for polystyrene panels [11] and reinforced geopolymer concretes [12, 13]. However, the main drawbacks of such newly produced alkali-activated binding material (geopolymer) are: high brittleness [14, 15], high shrinkage and low resistance to cracking [16]. Fiber reinforcement has been shown in several studies to be an effective strategy for improving mechanical performance, shrinkage control, and cracking prevention. The fibers incorporation controls debonding, sliding and fracture toughness [17, 18 a&b]. The target of the current study is to investigate the effect of various ratios of steel fiber on the performance of slag geopolymer composite.

*Corresponding author e-mail: chemist-sara@hotmail.com.; (Sara Moied)

Receive Date: 24 July 2022, Revise Date: 31 August 2022, Accept Date: 04 September 2022,

First Publish Date: 04 September 2022

DOI: 10.21608/EJCHEM.2022.152078.6590

©2022 National Information and Documentation Center (NIDOC)

2. Experimental.

2.1. Materials.

Ground granulated blast furnace slag (GGBFS) was used as a source of aluminosilicate for the synthesizing of geopolymer composites in this work, accordingly investigated by the X-Ray Fluorescence technique (XRF) to determine the chemical composition and the oxides were given in Table (1).

Table (1): Chemical composition of water-cooled slag (GGBS), %.

Oxide content (%)	SiO ₂	Al ₂ O ₃	Fe ₂ O ₃	CaO	MgO	SO ₃	K ₂ O	Na ₂ O	TiO ₂	MnO	P ₂ O ₅	Cl	SrO	BaO	L.O.I.	Total
Water - Cooled Slag (GGBFS)	36.67	10.31	0.50	38.82	1.70	2.17	1.03	0.48	0.57	4.04	0.04	0.050	0.18	3.28	0.12	99.96

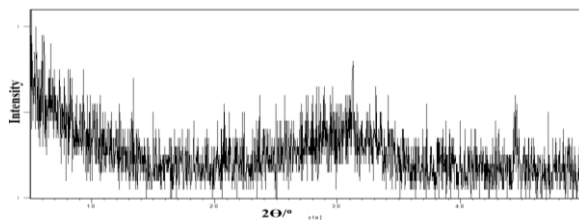


Fig.(1): X-Ray diffraction pattern of the starting raw materials.

The mineralogical composition of the raw material (GGBFS) showing its amorphous structure, illustrated in Fig (1).

In spite of various fiber types used in reinforcing geopolymer composites, steel fibers are still the most useable type [19], especially short wave-shaped (crimped) steel fiber which used in this study as shown in Fig (2). Mechanical and physical characterization of the steel fiber are presented in ASTM A820 [20]. Steel fibers, in particular, make a very strong link with the geopolymer composite. This strong bond can be aided by high bearing resistance, such as that provided by length-deformed steel fibers, which results in extremely high fiber-matrix bond strength.

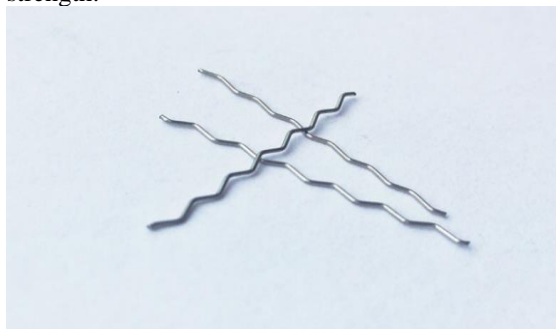


Fig. (2): visual image of used steel fiber.

2.2. Preparation of Geopolymer Mixtures.

Raw materials were ground to particle size passing a 90 μm sieve. The alkaline activator was made by dissolving sodium hydroxide pellets in mixing water and stirring thoroughly, then allowing the solution to cool for a sufficient period until it reaches room temperature because of the heat generated by melting sodium hydroxide. In a pan mixer, the alkaline

activator NaOH solution was gently added to dry powder and mixed for 5 minutes to ensure homogeneity. According to standard specification [21], the water-to-binder ratio (w/b) for all mixtures was measured and listed in table (2). The amount of water in the geopolymer mixture is important since it influences the quality and properties of the yielded geopolymer. [22].

The mould with dimensions of 2.5×2.5×2.5 cm was lubricated firstly, to avoid the specimen from being broken while demoulding, the paste was poured inside then compacted manually. After ending the casting, the moulds were covered and left till complete drying at room temperature (23°C) for 24 hrs, demoulded and kept in a fog room at 38°C and 90% relative humidity.

Table (2): composition of geopolymer mixtures, %.

Mix	BFS, %	Steel fibre %	Water/binder ratio
1	100	0	0.21
2	100	0.5	0.21
3	100	1	0.21
4	100	2	0.22
5	100	3	0.22

2.3. Techniques And Apparatus.

Fourier transformed infrared spectrometer (FTIR) spectrum of a compound can be used as a finger print to provide qualitative and quantitative analysis of a solid. In the present study, infrared spectral analysis has been carried out on selected specimens by Jasco-6100 to provide information about the reaction products. Test samples were ground and uniformly mixed with KBr at a weight ratio KBr: specimen=200:1. The mixture, about 0.20 g was pressed to a disk of 13 mm in diameter for analysis at 8 t/cm². The wavenumber was ranging from 400 to 4000 cm⁻¹ [23]. The chemical analysis of raw material was carried out using the X-Ray Fluorescence (XRF) technique for which an Axios, WD-XRF (PWY 400) Sequential Spectrometer (Panalytical, Netherland, 2009). The amorphous phases present in the geopolymer specimens were detected by the X-ray diffraction (XRD) technique using a Cu-K α source (Philips PW105170) in range from 0 to 50 2 θ . According to ASTM C109, compressive strength measurements were performed using a five-ton German Brüf pressing machine with a loading rate of 100 kg/min. Drying shrinkage was measured through measuring the wet length of the test specimen and then placed in dryer at 105°C for 24±2 hrs, measuring the dry length and calculating the drying shrinkage after the elapse of different time periods.

3. Results and Discussion

3.1. FTIR Technique.

The FTIR patterns of slag geopolymer activated by 6% NaOH and reinforced with steel fiber with different ratios (0, 0.5, 2, and 3 %) as addition percentage cured at 90 days presented in Fig. (3). as shown from the graph the unique peak at about 950-1000 cm^{-1} which is the fingerprint of the geopolymerization [24] is associated with (Al-O) and (Si-O) asymmetric stretching vibrations. It was found out that the absorption bands of WCS geopolymer are: Both (asymmetric and symmetric) stretching vibrations of the octahedral OH bonds linked to the Al octahedron sheet were indicated by absorption bands in the 3400-3500 cm^{-1} range, whereas the absorption band at about 1645 cm^{-1} was attributed to the bending vibrations of (H-O-H) [25]. The significant absorption band located at 1433 cm^{-1} is due to the CO_3^{2-} stretching vibrations. Meanwhile, the dispersion of atmospheric carbonate inside the composites during the ageing process produced the development of the absorption band [26]. The band at 954 cm^{-1} was caused by the asymmetric stretching vibrations of (Si-O-T) where (T, tetrahedral =Si or Al) [27]. The other bands signifying the main geopolymer bonds (Si-O-Si and Si-O-Al) at the range of 470- 893 cm^{-1} [28]. The position of characteristic peak for pure silica spectra at 1100 cm^{-1} this displacing to $\sim 1013 \text{ cm}^{-1}$ for the studied composites probably causing by Al^+ atoms in tetrahedral coordination influence a shift band to lower wavenumbers [29,30].

The FTIR patterns concluded that the intensity of asymmetric band Si-O-Al is almost constant up to 2% of steel fiber inclusion, this increase may be as a result of nucleation effect of steel fiber forming 3D geopolymer framework [31,32]. However, by the rise of steel fiber ratio there is a degradation to the band has been occurred may be attributed to segregations to the reacting particles as a reversing effect. Meanwhile, the intensity of hydration bands of almost equal intensity indicating formation of CSH, CASH beside NASH as well as NCASH.

For confirming the optimum ratio and the previous results, the Fig. (4) Illustrated the slag geopolymer composites reinforced with 2% steel fiber at different curing times up to 90 days. The pattern concluded that the growth of hydration bands with time attributing to increasing CSH and NASH as geopolymerization reaction with curing age proceeds. Furthermore, worthy noticed the splitting of carbonate bands at about 1464 cm^{-1} is likely related to the distorted nature of CO_3^{2-} minerals at early ages where the bands turned to be dense at later ages. Asymmetric Si-OH vibrations at 840 cm^{-1} , symmetric stretching vibrations (Si-O-Si) at 676-700 cm^{-1} , and bending vibrations (Si-O-Si and O-Si-O) at 430-445 cm^{-1} have also been identified. The

spectra of all mixtures revealed the presence of typical O-H stretching vibration as exhibited by a broad absorption band around 3450 cm^{-1} as well as bending vibration centered at 1645 cm^{-1} indicate to crystalline H_2O of the hydrated products such as CSH and CAH. The quantity of tetrahedral aluminium atoms increases as the geopolymerization process improves, causing bands to shift to lower wavelengths [33] this shift happens due to the formation of aluminosilicate gel [34].

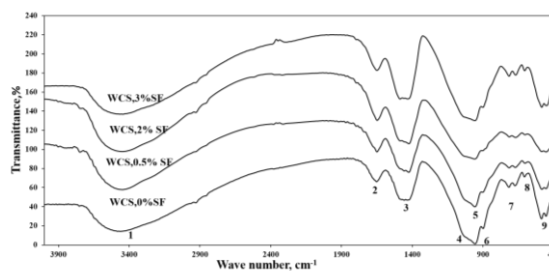


Fig (3) FTIR spectra of geopolymer composites reinforced by (0, 0.5, 1 and 3%) steel fiber cured at 90 days. [1: stretching vibration of O-H, 2: Bending vibrations of (HOH), 3: Stretching vibration of CO_2 , 4: Asymmetric stretching vibration (Si-O-Si), 5: Asymmetric stretching vibration (T-O-Si), 6: Symmetric stretching vibration CO_2 , 7, 8: Symmetric stretching vibration (Si-O-Si), 9: Bending vibration of (Si-O-Si)].

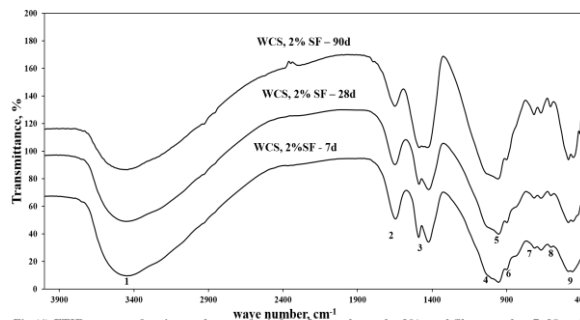


Fig (4) FTIR spectra of optimum dosage of reinforced geopolymer by 2% steel fiber cured at 7, 28 and 90 days. [1: stretching vibration of O-H, 2: Bending vibrations of (HOH), 3: Stretching vibration of CO_2 , 4: Asymmetric stretching vibration (Si-O-Si), 5: Asymmetric stretching vibration (T-O-Si), 6: Symmetric stretching vibration CO_2 , 7, 8: Symmetric stretching vibration (Si-O-Si), 9: Bending vibration of (Si-O-Si)].

3.2. X-Ray Diffraction Analysis.

By the way for well studying the geopolymer composites microstructural properties, XRD technique utilized. A broad hump, which is characteristic of amorphous geopolymers, was shown in geopolymers between 18 and 36° 2 θ [35]. Accordingly, Fig. (5) exhibited the XRD pattern of slag-based geopolymer composites reinforced with steel fiber by different ratios as 0, 0.5, 2 and 3% cured at 90 days. The patterns show that the predominant phases are CSH and Sodalite (Na Al Silicate hydroxide hydrate) beside traces from Akermanite (CaMgSilicate), Reversedite, Hematite as well as quartz crystalline phases. Likewise, it is worthy distinguished a rise between 20 and 33° in 2 θ , which is a typical manners in amorphous materials [36] which evidenced almost of equal intensity up to 2% steel fiber [37]. The pattern reflects that by adding steel fiber the crystalline phase existing in raw material gradually decrease forming amorphous phases as CSH attributed to the nucleation effect of steel fiber for the geopolymer network forming three-dimensional network [38,39]. As the steel fiber ratio

exceeds 2% the peak intensity gradually reduced as a result to lowering in the strength.

Then again, Fig (6) presented the XRD pattern of the effect of enhancing the geopolymer with a ratio 2% of steel fiber with curing time up to 90 days. The pattern concluded that as a hump peak increase is an indication of geopolymer network enhancement moreover, forming CSH as well as NASH. There is a slight elimination to the Akermanite phases resulted in MgAlSilicate phases presence which strengthen the geopolymer network.

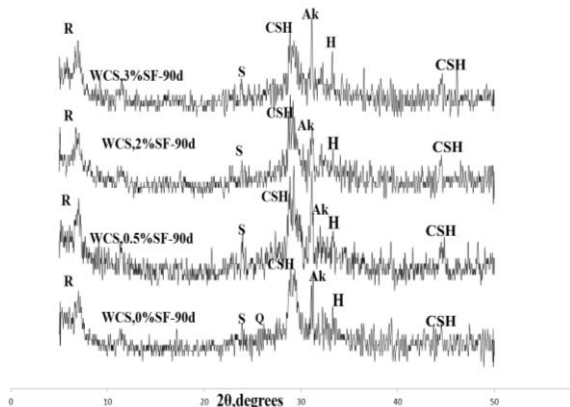


Fig (5) XRD pattern of geopolymer composites reinforced by different ratio of steel fiber cured at 90 days. [R:Reverse dicit,CSH: Calcium Silicate Hydrate, S:Sodalite, Q:Quartz, Ak:Akermanite and H:Hematite]

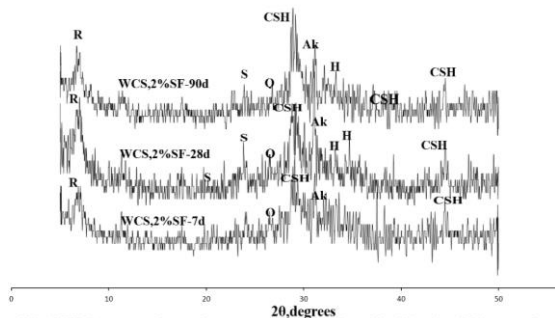


Fig (6) XRD pattern of geopolymer composites reinforced by 2% of steel fiber cured at 7,28 and 90 days. [R:Reverse dicit,CSH: Calcium Silicate Hydrate, S:Sodalite, Q:Quartz, Ak:Akermanite and H:Hematite]

3.3. Water Absorption.

The physical properties (water absorption) investigated for the slag geopolymer composites reinforced by various ratios (0.5, 2 and 3%) of steel fiber respectively comparing with unreinforced slag geopolymer then the results strategized graphically in a function of the curing time in Fig.(7). The values of water absorption of starting raw material (water-cooled slag) at 28 days is 9.7 % , and this is almost constant with the incorporation of steel fiber by various ratios 0.5, 2 and 3 to be 9.62, 9.48 and 9.60 respectively. Consequently, the geopolymer composites become less permeable to water owing to the pore is been occupied by addition of the steel fiber which slightly beneficial to fill voids and pores. This growth is almost constant till 2% of sf, as the sf content exceeds the water absorption gradually increase. Due to the ability of the fibers themselves to

reduce the quantity of water absorbed by the matrix, the presence of fibres showed a minor improvement in lowering water absorption. [40].

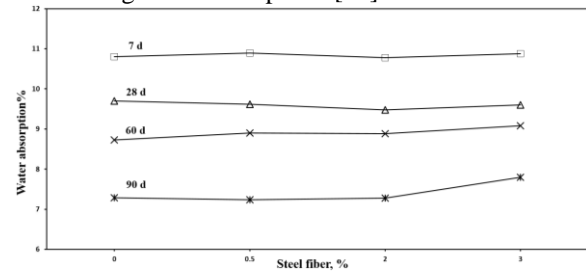


Fig (7) variation of water absorption of geopolymer composites reinforced by different ratio steel fiber cured at 7, 28, 60 and 90 days

3.4. Shrinkage.

The use of fiber-reinforced geopolymer as an important technical measure to tackle the shrinkage problem has been recommended by many researchers. While the microfibers in geopolymer composites are expected to effectively dominate shrinkage and cracking, steel fiber was shown to be more successful in limiting drying shrinkage, with a decrease rate of about 40% [41]. Figure (8) illustrates the shrinkage behavior of geopolymer composites reinforced with 0.5,2 and 3 % of steel fiber comparing with the neat slag geopolymer. The pattern shows that inclusion of sf till 2% controlled the drying shrinkage may be attributed to stiffness of the fibers and contact interface to the geopolymer matrix. Above this ratio, drying shrinkage increases significantly due to difficulties in vibration and compaction, resulting in negative impacts of fiber incorporation on specimen shrinkage control as the strong interface contact between steel fiber and the geopolymer matrix, as well as the greater Young's modulus of the fiber, shrinkage was controlled by lowering the fiber inclusion. [42].

Ye et al, suggested that this reversal of behavior could be due to the introduction of alkali metal cations into the C-A-S-H structure, resulting in a decrease in the accumulation of the C-A-S-H layer, followed by collapse and redistribution of the layer due to internal pressures generated by drying [43].

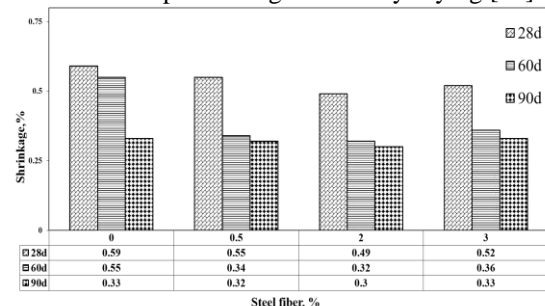


Fig (8): variation of shrinkage of WCS geopolymer composites reinforced by different ratio steel fiber cured at 28, 60 and 90 days.

3.5. Compressive Strength Results.

By studying the compression test of geopolymer composites reinforced with several steel fiber ratios and be represented at Fig. (9). Based on the results,

the steel fiber inclusion contribute in enhancing the compressive strength values that may be due to increasing geopolymer density and compaction as steel fiber content increase or because of orientation of steel fiber is randomly and homogenous meanwhile arrest cracks formation and propagation thus, promote strength of the geopolymer [44]. The values of the compressive test on cube specimens according to test standard are shown in Fig.(9) which Illustrated that the strength slightly decreased at early ages due to incomplete dissolution of silicon and aluminum oxides from the raw material while upon increasing the curing time and in the presence of NaOH, Si, Al and Ca ions leached out from the starting materials and with incorporating of the steel fibers the compressive strength with almost a steady-state sequence increase as increasing the ratio of steel fiber added till the 2% after this ratio the strength slightly decrease, This is due to the filler effect of the fine particles of water-cooled slag which are capable to spread the filler and pozzolanic effects. The results were confirmed by FTIR as well as XRD were almost the main asymmetric stretching vibration of geopolymer at about 980 cm⁻¹ almost of steady-state up to 2% then exposed to a decrease in broadness as well as intensity leading to strength loss.

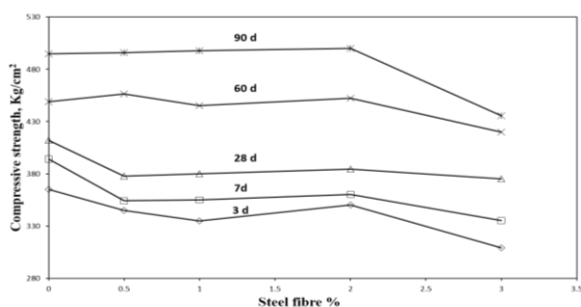


Fig (9) compressive strength of geopolymer composites reinforced by steel fiber at curing time 3,7,28,60 and 90 days

4. Conclusions.

This paper presents the findings of an experimental study on slag-based geopolymer composites reinforced by various steel fiber ratios, from which the following conclusions can be drawn:

1. Utilizing granulated blast furnace slag is an eco-friendly alternative binder to Portland cement in terms of applications and research.
2. The enclosure of fibers healing the micro-cracks within the matrix enhances the ductility and the durability of the geopolymer.
3. The inclusion of fibers into geopolymer composites enhances mechanical and physical properties.
4. The steel fibers are appropriately small to be well dispersed in an unhardened geopolymer mixture.
5. As steel fiber content and age growth of the mixes increase affecting positively on the compressive strength results, it is also drawn

that, the shrinkage cracking related with the alkaline activation of slag reduces as the fiber content increases.

6. The optimum ratio for reinforcing the slag-based geopolymer composites activated by 6% NaOH is up to 2% of steel fiber by weight.

5. Declaration.

***Conflict of interest:** The authors declare that they have no known competing financial interests or personal relationships that could have appeared to influence the paper.

***Availability of data and material:** All data generated or analysed during this study are included in this published article and its supplementary information files.

***Funding:** There is no source of funding for the current paper.

***Ethics approval and consent to participate:** “Not applicable” in this section.

***Consent for publication:** Not applicable” in this section.

6. References

1. Punuraia, W.; Kroehongb, W.; Saptamongkolb, A.; Chindaprasirt, P., “Mechanical properties, microstructure and drying shrinkage of hybrid fly ash-basalt fiber geopolymer paste”, *Construction and Building Materials*,186,62-70,2018.
2. Xu, M.; He, Y.; Wang, C.; He, X.; He, X.; Liu, J. ; Cui, X., “Preparation and characterization of a self-supporting inorganic membrane based on metakaolin-based geopolymers”, *Applied Clay Science*, 115,254-259,2015.
3. Khater, H.M.; Ezzat, M.; El Nagar, Abdeen M., “Engineering of low cost geopolymer building bricks applied for various construction purposes”, *International Journal of civil engineering and technology*, july, 7(4):81-99, 2016.
4. Khater, H.M.; M. Ezzat, “Preparation and characterization of engineered stones based geopolymer composites”, *journal of building engineering*, 20; 493-500, 2018.
5. Khater, H.M., “Valorization of cement kiln dust in activation and production of hybrid geopolymer composites with durable characteristics”, *Advanced composites and hybrid materials*, springer, DOI 10.1007/s42114-019-00097-5, 2019.
6. Pacheco-Torgal, F.; V.Abdollahnejad;; A.F.Camões.; M. Jamshidi.; Y. Ding., “Review, “Durability of alkali-activated binders: A clear advantage over Portland cement or an unproven issue”, *Construction and Building Materials*,30,400–405,2012.

7. Khater, H.M., "Studying the Effect of Thermal and Acid Exposure on Alkali Activated Slag Geopolymer", *Advances in Cement Research*, 26,1: 1–9,2014.
8. Bernal S.; Rodriguez E, mejia de Gutierrez R, Maldonado J., "Durabilidad de Concretos de Escoria Siderurgica Activada Al calinamente". In: *Proceedings 1er Coloquio de Investigacion en materiales no Conven Cionales Brasil-Colombia, Cali-Colombia, 2005*.
9. Liang, G.W.; Li, H.X.; Zhu, H.J.; Liu, T.J.; Chen, Q.; Guo, H.H., "Reuse of waste glass powder in alkali-activated metakaolin/fly ash pastes: Physical properties, reaction kinetics and microstructure" *Resource Conserved Recycling*, 173, 105721, 2021.
10. Arulrajah, A.; Kua, T.-A.; Horpibulsuk, S.; Phetchuay, C.; Suksiripattanapong, C.; Du, Y.-J., "Strength and microstructure evaluation of recycled glass-fly ash geopolymer as low-carbon masonry units" *Construction Building Materials*, 114, 400-406, 2016.
11. Phoo-neg, T.; Hanjitsuwan S.; Ridtirud, Ch.; Sata, V., "Compressive strength, Bending and Fracture Characteristics of High Calcium Fly Ash Geopolymer Mortar Containing Portland Cement Cured at Ambient Temperature", *Arabian journal for Science and Engineering*, 41, 4, 2015
12. Mo, K.H.; Alengaram, U.J.; Jumaat, M.Z., "Structural performance of reinforced geopolymer concrete members: a review" *Construction Building Materials*, 120, 251-264, 2016.
13. Visintin, P.; Mohamed Ali, M.S.; Albitar, M.; Lucas, W., "Shear behaviour of geopolymer concrete beams without stirrups" *Construction Building Materials*, 148, 10-21, 2017.
14. Pan, Z.; Sanjayan, J.G.; Rangan, B.V., "Fracture properties of geopolymer paste and concrete", *Mag. Concr. Res.* 63, 10, 763–771, 2011.
15. Sarker, P.K.; Haque, R.; Ramgolam, K.V., F, "fracture behaviour of heat cured fly ash based geopolymer concrete", *Mater. Des.* 1, 44, 580–586, 2013.
16. Khan, M.Z.; Hao, Y.; Hao, H.; Shaikh, F.U., "Mechanical properties of ambient cured high strength hybrid steel and synthetic fibers reinforced geopolymer composites", *Cem. Concr. Compos.* 1, 85, 133–152, 2018.
17. Collins F., Sanjayan, J.G., "Microcracking and strength development of alkali activated slag concrete". *Cement and Concrete Composites*; 345:52- 23(4);, 2001.
- 18(a). Silva, F.J. C. Thaumaturgo, "Fiber reinforcement and fracture response in geopolymeric mortars", *Fatigue & Fracture of Engineering Materials & Structures*; 26:167–72, 2003.
- 18(b). Silva, F.J.; Thaumaturgo, C., "The chemistry, reinforcement and fracture in geopolymeric cement composites". *International: Proceedings of the 11th international congress on the chemistry of cement (ICCC). Cement's contribution to the development in the 21st century, Durban – South Africa*; 1379–87, 2003.
19. Bhutta A; Borges, P.H.R.; Zanotti, C.; Farooq, M. Banthia, N., "Flexural behavior of geopolymer composites reinforced with steel and polypropylene macro fibers" , *Cement and Concrete Composites* ,80,31-40,2017.
20. Han, B.; Yu, X.; Ou, J., "Compositions of Self-Sensing Concrete", *Self-Sensing Concrete in Smart Structures*; 13-43; 2014.
21. ASTM C187, "Standard Test Method for Amount of Water Required for Normal Consistency of Hydraulic Cement Paste", 2016.
22. Khater, H.M., "Effect of cement kiln dust on Geopolymer composition and its resistance to sulphate attack", *green material journal*,; 1,1,36-46, 2013.
23. Lizcano, M.; Gonzalez, A.; Basu, S.; Lozano, K.; Radovic, M., "Effects of water content and chemical composition on structural properties of alkaline activated metakaolin based geopolymers", *J. Am. Ceram. Soc.* 95, 2169–2177, 2012.
24. Chindapasirt P, Rattanasak, Jaturapitakkul. U, "Utilization of fly ash blends from pulverized coal and fluidized bed combustion in geopolymeric materials", *Cement Concrete Composition*, 33:55-60, 2011.
25. Panias, D.; Giannopoulou, I.P.; Perraki, T. "Effect of synthesis parameters on the mechanical properties of fly ash-based geopolymers", *Colloids and Surfaces A: Physicochemical and Engineering Aspects*, 301, 246-254, 2007.
26. Wan, O.; Heah, Y; Cheng-Yong Mohd Mustafa Al Bakri Abdullah Long-Yuan Li Li Ngee Ho Foo Kai Loong Ong Shee-Ween Ng Hui-Teng Ng Yong-Sing Nur Ain Jaya, "Comparative mechanical and microstructural properties of high calcium fly ash one-part geopolymers activated with Na₂SiO₃-anhydrous and NaAlO₂", 15, 3850-3866, *Materials Research and Technology*, 2021.
27. Askarian M, Tao Z, Samali B, Adam G, Shuaibu R. Mix composition and characterization of one-part geopolymers with different activators. *Construction and Building Materials*; 225:526e37, 2019.
28. Criado M, Fernandez-Jimenez A, Palomo A. "Alkali activation of fly ash: effect of the SiO₂/Na₂O ratio: Part I: FTIR study",

- Microporous and Mesoporous Materials; 106(1e3):180e91, 2007.
29. Zhang, J.; Provis, J.L.; Feng, D.; van Deventer, J.S.J., "Geopolymers for immobilization of Cr6+, Cd2+, and Pb2+", *Journal of Hazardous Materials*, 157, 2–3, 587-598, 2008.
 30. Lee, W.K.W.; Van Deventer, J.S.J. "Use of Infrared Spectroscopy to Study Geopolymerization of Heterogeneous Amorphous Aluminosilicates", *Langmuir* 19, 8726, 2003.
 31. Wallah, S.E.; Rangen, B.V., "Low- calcium fly ash-based geopolymer concrete long term properties", Resresearch Report GC₂, Faculty of Engineering Curtin University of Technology Perth, Australia, 2006.
 32. Khater, H.M, "Optimization of geopolymer mortar incorporating heavy metals in producing dense composites", *Journal of Building engineering*, 32, 101684, 2020.
 33. Autef, A.; Joussein, E.; Poulesquen, A.; Gasgnier, G.; Pronier, S.; Sobrados, I.; Sanz, J.; Rossignol, S., "Influence of metakaolin purities on potassium geopolymer formulation: the existence of several networks", *J. Colloid Interface Science*, 408, 43–53, 2013
 34. Rees, C.A.; Provis, J.L.; Lukey, G.C.; Deventer, J.S.J., "Attenuated total reflectance fourier transform infrared analysis of fly ash geopolymer gel aging", *Langmuir*, 23 8170–8179, 2007.
 35. Arioz, E.; Arioz, O.; Mete Kockar, O., "An experimental study on the mechanical and microstructural properties of geopolymers", 20th International Congress of Chemical and Process Engineering CHISA 2012, 25 – 29 Prague, Czech Republic, 2012, *Procedia Engineering* 42, 100 – 105, 2012.
 37. Achile, N.; Noela, E.; Kaze, C.; Rodrique, J.; Giogetti, N.; Deutou, J.; Noel, Y.; Djobo, S.; Tomé, T.; Salman, A.; Jean, N.; Elie, K.; Cristina, L., "Mechanical strength and microstructure of metakaolin/volcanic ash-based geopolymer composites reinforced with reactive silica from rice husk ash (RHA)", *Journal of Materialia*, 16, 101083, 2021.
 39. Khater, H.M; El-nagar, A.M., "sustainable production of eco-friendly MwCNT geopolymer composites with superior sulfate resistance", *Advanced composite and hybrid materials*, Springer; 3:375-389, sep 2020.
 40. Celik A.; Yilmaz, K., Canpolat O., M. Al-mashhadani M.; Aygörmez Y.; Uysal M., "High-temperature behavior and mechanical characteristics of boron waste additive metakaolin based geopolymer composites reinforced with synthetic fibers", *Construction and Building Materials*, 187, 1190-1203, 2018.
 41. Lyu, B.; Ding, C.; Guo, L.; Chen, B.; Wang, A., "Basic performances and potential research problems of strain hardening geopolymer composites": A critical review; *Construction and Building Materials*, 287, 123030, 2021.
 42. Ranjbar, N.; Talebian, S.; Mehrali, M.; Kuenzel, C.; Metselaar, H. S. C., Jumaat M. Z., "Mechanisms of interfacial bond in steel and polypropylene fiber reinforced geopolymer composites", *Composites Science and Technology*, Volume 122, 73-81, 2016.
 43. Ye, H.; Radlinska, A. "Shrinkage mechanisms of alkali-activated slag", *Cement and Concrete Research*, 88, 126–135, 2016.
 44. Abdullah, M.; Faris, M.; Tahir, M., Kadir, A.; Sandu, A., Mat, Isa, N.; Corbu, O. "Performance and Characterization of Geopolymer Concrete Reinforced with Short Steel Fiber", *IOP Conference Series: Materials Science and Engineering*, 2017.